

# Analytical Method of Submarine Buried Steel Pipelines Under Strike-slip Faults

**X. Li, B. Wang, J. Zhou**

*State Key Laboratory of Coastal and Offshore Engineering, Dalian University of Technology, China*



## **SUMMARY:**

To study the response of subsea buried steel pipelines surrounded by homogeneous site soils subjected to active strike-slip faults more accurately, an improved analytical methodology herein has been proposed by considering the nonlinear constitutive models of pipe steel and pipe-soil interaction. Based on the beam-on-elastic-foundation and elastic-beam theories, the pipe maximum axial total stress and strain are derived. Compared with Karamitros method, the pipe maximum axial total strains from the proposed analytical methodology are in better agreement with ones from the finite element analysis, and suitable for engineering applications due to conservative results.

*Key words: strike-slip fault; submarine buried steel pipeline; nonlinear pipe-soil interaction; beam on elastic foundation; elastic beam*

## **1 INTRODUCTION**

Submarine pipelines have been used extensively in ocean engineering and are regarded as the lifelines of offshore oil and gas fields. The Bohai Sea and East China Sea are seismically active regions in China. Sea bed deformation during earthquakes, such as dune movement, settlement, landslide, fault movement, and debris flow, is one of the potential reasons for submarine buried pipeline damage. It is of great significance to study the seismic failure mechanism of submarine buried pipelines subjected to fault movements.

Modern numerical techniques based on finite element method (FEM) were used to solve the problem by Liu et al. (2008), Gu et al. (2009), Jiao et al. (2009) and Vazouras et al. (2010). Nevertheless, the numerical techniques have not been introduced into the pipeline design codes. Moreover, the simplified analytical models still provides a basis for preliminary design and verification of more complicated numerical models.

Applying a small-displacement model with static soil pressure and static friction force, Newmark and Hall (1975) proposed an analytical method to study the effects of fault displacements on buried steel pipelines. Later, based on the assumption of a circle arc model, Kennedy et al. (1977) extended Newmark and Hall's procedure and simulated a pipe as a cable with tension stiffness and no flexural stiffness. Wang and Yeh (1985) simplified a pipe subject to fault movements into a large-deformation beam with constant curvature and a beam on elastic foundation. Due to the constant curvature large-deformation beam model adopted, both of Kennedy and Wang methods overestimated the effect of soil resistance on pipe bending strain. Karamitros et al. (2006) improved the work of Wang and Yeh by using the elastic beam instead of the constant curvature large-deformation beam and considering the actual distribution of stresses on the pipeline cross-section and the compatibility requirement of the shear force at the conjunction of elastic beam and its neighboring beam on elastic foundation. The analytical method neglected the nonlinearity of pipe-soil interaction.

Adopting the Ramberg-Osgood stress-strain relationships for pipe steel and the soil-pipeline nonlinear interaction models referred to American Lifeline Alliance (ALA) (2001), an improved analytical methodology of submarine buried steel pipelines surrounded by homogeneous site soils subjected to active strike-slip faults is proposed in this paper. The effect of axial force on flexural stiffness is considered with the clear physical meaning.

## 2 CONSTITUTIVE MODELS

### 2.1 Ramberg-Osgood stress-strain relationships of pipe steel

To consider material nonlinearity of pipe steel, the Ramberg-Osgood model is selected to simulate the elastic-plasticity properties of pipe steel. The expression of the Ramberg-Osgood model is:

$$\varepsilon_x = \frac{\sigma_x}{E_0} \left[ 1 + \frac{n}{1+r} \left( \frac{\sigma_x}{\sigma_y} \right)^r \right] \quad (2.1)$$

$$E_{\tan,x} = \frac{d\sigma_x}{d\varepsilon_x} = \frac{E_0 \sigma_y^r}{\sigma_y^r + n \sigma_x^r} \quad (2.2)$$

where  $\varepsilon_x$  and  $\sigma_x$  are the engineering strain and stress;  $E_0$  is the initial Young's modulus;  $\sigma_y$  is the yielding stress of pipe material;  $n$  and  $r$  are the Ramberg-Osgood parameters; and  $E_{\tan,x}$  is the tangent Young's modulus. Since the tangent modulus is monotonic decreasing with increasing engineering stresses, subsequent nonlinear iteration procedure due to the difference of the Young's modulus in each iterative step is assured to converge definitely.

### 2.2 Pipe-soil nonlinear interaction

The pipe-soil nonlinear interactions in the axial and lateral directions are simulated as the elastic perfectly-plastic soil springs recommended by ALA.

## 3 SOLUTION ALGORITHM

### 3.1 Description of problem

The strike-slip fault is simplified as an inclined plane, i.e. with null width of rupture zone. As earthquake is a small probability event, the consolidation of backfilled soil has completed. Based on the concept originally introduced by Wang and Yeh (1985), the pipeline is divided into four segments displayed in Figure 1. Only half of the pipe structure (segment A'B) is analyzed due to the anti-symmetric deformation of submarine buried pipeline under a strike-slip fault. In Figure 1, point B is the intersection of the pipeline axis with the fault trace, where the bending moment equals to zero, while points A and C are the closest points of the pipeline axis from point B with zero lateral pipe-soil relative displacement. Points A' and C' are at a distance from points A and C that is sufficient for the attenuation of lateral pipe-soil relative displacements.

The fault movement is defined in a Cartesian coordinate system, where the  $x$ -axis is parallel to the longitudinal axis of the undeformed pipeline, the  $y$ -axis is perpendicular to  $x$  in the horizontal plane, and  $\beta$  is the crossing angle of the fault trace and the  $x$ -axis (Figure 1). The crossing angles applied in the paper is limited in the range  $0 < \beta < 90^\circ$ , which results in pipeline elongation. In Figure 1,  $\Delta_f$  is the fault displacement. The intersection B moves one-half of  $\Delta_f$ .  $\Delta X$  and  $\Delta Y$  are respectively the axial and lateral components of fault displacements in one side of fault.  $L_C$  is the length of the

pipe-soil large deformation segment in one side of fault.  $f_L$  and  $q(x)$  are the axial and lateral soil spring forces per unit length of pipeline, respectively.

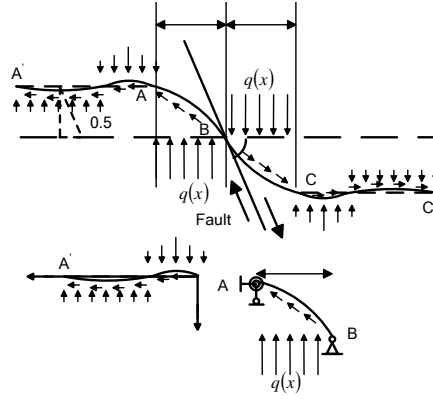


**Figure 1.** Partitioning of buried pipelines due to strike-slip faults

### 3.2 Axial response analysis of pipeline

Geometrical elongation of pipeline is the pipe deformation obtained from geometrical compatibility conditions under fault movements. The geometrical elongation of pipe  $\Delta L_{\text{geo}}$  is:

$$\Delta L_{\text{geo}} = \Delta X + \frac{\Delta Y^2}{2L} \approx \Delta X = \frac{1}{2} \Delta_f \cos \beta \quad (3.1)$$

where  $L$  is the pipe unanchored length defined as the pipe length where relative slippage occurs between the pipe and the surrounding soil. As  $\frac{\Delta Y^2}{2L}$  is much less than  $\Delta X$ , the geometrical elongation provoked by the lateral fault displacement component  $\Delta Y$  may be neglected.

Physical elongation of pipeline is the pipe deformation resulting from the integration of axial strain along the unanchored length of pipe. The physical elongation of pipe  $\Delta L_{\text{phy}}$  is:

$$\Delta L_{\text{phy}} = \int_0^L \varepsilon_{\text{ax}} dL \quad (3.2)$$

where  $\varepsilon_{\text{ax}}$  is the axial strain of arbitrary point along the unanchored length.

According to the axial soil reaction along the unanchored pipeline, two cases are classified. For case 1, soil reaction is proportional to the relative pipe-soil displacement, indicating that soil springs are in elastic state; for case 2, soil reaction reaches to the limit value, representing that part of soil springs has yielded.

#### 3.2.1 Elastic case for axial soil springs

In Figure 2, point O is the closest point of the pipeline axis from the intersection B with zero axial pipe-soil relative displacement,  $L$  is the pipe unanchored length, point P is the hypothetical point where the axial soil spring just yields, and  $L_0$  is the pipe maximum length of the elastic segment of axial soil springs. The pipe elongation of segment OP is  $u_0$ , which is the yielding displacement of axial soil spring, i.e. the pipe-soil axial relative displacement of point P is  $u_0$ . Since the axial soil

springs are still elastic along the pipeline, the pipe elongation of segment  $L$  is less than or equal to the yielding displacement of axial soil spring, i.e.  $\Delta X \leq u_0, L \leq L_0$ .

The axial soil spring force per unit length of pipe assumed to change linearly along segment  $L_0$  is expressed as

$$f_L = \begin{cases} f_s \frac{x}{L_0} & (0 \leq x \leq L_0) \\ f_s & (x \geq L_0) \end{cases} \quad (3.3)$$

where  $f_s$  is the maximum axial soil spring force per unit length of pipe.

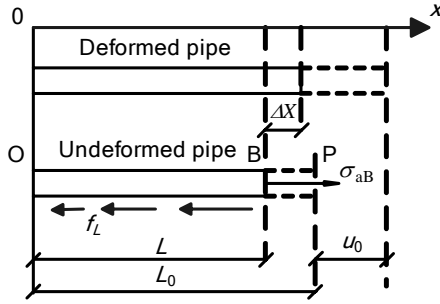


**Figure 2.** Pipe axial elongation of unanchored segment with axial soil springs not yielding

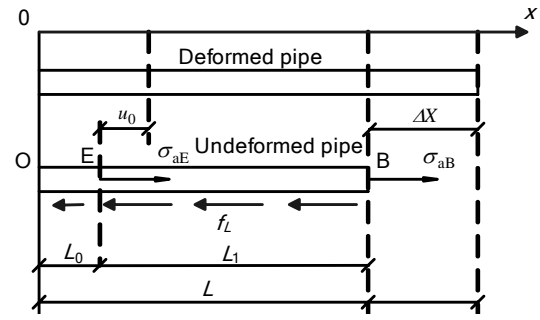


**Figure 3.** Pipe axial elongation of unanchored segment with axial soil springs yielding

Then, the axial stress at the intersection of the pipeline with the fault trace  $\sigma_{aB}$  is:

$$\sigma_{aB} = \frac{1}{A_s} \int_0^L f_L dx = \frac{f_s L^2}{2A_s L_0} \quad (3.4)$$

where  $A_s$  is the area of pipeline cross-section,  $A_s = \frac{1}{4} \pi (D^2 - d^2) = \pi (D - t)$ ,  $t$  is the wall thickness of pipe,  $D$  and  $d$  are respectively the pipe external and internal diameters.  $L_0$  can be obtained by the relation that the pipe physical elongation of segment  $L_0$  equals to  $u_0$ , while  $L$  can be determined by the relation that physical elongation of pipeline equals to the geometrical one. Namely:

$$u_0 = \frac{f_s L_0^2}{2A_s E_0} \left[ \frac{1}{3} + \frac{n}{(2r+3)(r+1)} \left( \frac{f_s L_0}{2A_s \sigma_y} \right)^r \right] \quad (3.5)$$

$$\Delta X = \frac{f_s L^3}{2A_s L_0 E_0} \left[ \frac{1}{3} + \frac{n}{(2r+3)(r+1)} \left( \frac{f_s L^2}{2A_s L_0 \sigma_y} \right)^r \right] \quad (3.6)$$

### 3.2.2 Yielding case for axial soil springs

For the axial soil springs yielding, the pipe elongation of segment  $L$  is larger than the yielding displacement of axial soil spring, i.e.  $\Delta X > u_0, L > L_0$ . To consider the axial pipe-soil nonlinear interaction, the unanchored pipeline is divided into two parts shown in Figure 3, namely,  $L_0$  and  $L_1$ . The axial soil springs of segment  $L_0$  keep elastic; while the axial soil springs of segment  $L_1$  yield totally. Point E is the critical point where the axial soil spring just yields.

The axial stress  $\sigma_{aE}$  at the conjunction point of segment  $L_0$  and  $L_1$  is:

$$\sigma_{aE} = \frac{1}{A_s} \int_0^{L_0} f_L dx = \frac{f_s L_0}{2A_s} \quad (3.7)$$

where  $L_0$  is obtained by solving Eq. (3.5).

The axial soil springs completely yield in the range  $L_0 \leq x \leq L$ , then,

$$L = L_0 + \frac{A_s}{f_s} (\sigma_{aB} - \sigma_{aE}) \quad (3.8)$$

The pipe physical elongation  $\Delta L_1$  of segment  $L_0 \leq x \leq L$  is:

$$\Delta L_1 = \frac{A_s \sigma_y^2}{f_s E_0} \left\{ \frac{1}{2} \left[ \left( \frac{\sigma_{aB}}{\sigma_y} \right)^2 - \left( \frac{\sigma_{aE}}{\sigma_y} \right)^2 \right] + \frac{n}{(r+1)(r+2)} \left[ \left( \frac{\sigma_{aB}}{\sigma_y} \right)^{r+2} - \left( \frac{\sigma_{aE}}{\sigma_y} \right)^{r+2} \right] \right\} \quad (3.9)$$

Since the pipe geometrical elongation equals to the pipe physical elongation, then

$$u_0 + \Delta L_1 = \Delta X \quad (3.10)$$

Substituting Eq. (3.9) into Eq. (3.10), the axial stress  $\sigma_{aB}$  at the intersection of the pipeline with the fault trace is obtained, and the pipe unanchored length  $L$  is calculated from Eq. (3.8).

### 3.3 Lateral response analysis of pipeline

#### 3.3.1 Segment AA' analysis

Based on the beam-on-elastic-foundation theory and the assumption that the Young's modulus of segment AA' is the initial Young's modulus for pipe steel due to the comparatively small deformation, the differential equilibrium equation of segment AA' on the basis of the  $xAy$  coordinate system shown in Figure 1 is taken as:

$$E_0 I y^{(4)} + k y = 0 \quad (3.11)$$

where  $y$  is the lateral pipe-soil relative displacement,  $k$  is the constant of the lateral soil spring,  $I$  is the moment of inertia of the pipeline cross-section,  $I = \frac{\pi}{64} (D^4 - d^4)$ .

According to the boundary conditions,  $y \rightarrow 0$  at  $x \rightarrow \infty$  and  $y = 0$  at  $x = 0$ , Eq. (3.11) is solved:

$$y = C_4 e^{-\lambda x} \sin(\lambda x) \quad (3.12)$$

where  $C_4$  is a constant, and  $\lambda = \sqrt[4]{\frac{k}{4E_0 I}}$ .

Due to  $V_A = -E_0 I y_A''''$ ,  $M_A = -E_0 I y_A''$  and  $\phi_A = y_A'$ , then

$$M_A = (2\lambda E_0 I)\phi_A, \quad V_A = -\lambda M_A \quad (3.13)$$

where  $\phi_A$ ,  $M_A$  and  $V_A$  are the rotational angle, the bending moment and the shear force at point A, respectively.

### 3.3.2 Segment AB analysis

Segment AB shown in Figure 4 is modeled as an elastic beam, supported at point A by a linear elastic rotational spring whose constant is calculated from Eq. (3.13) as  $C = 2\lambda E_0 I$ . A uniformly distributed load  $q$  is assumed to express the action of lateral soil springs.

$$q = \begin{cases} k\Delta Y & \Delta Y \leq \Delta_p \\ q_u & \Delta Y > \Delta_p \end{cases} \quad (3.14)$$

where  $q_u$  is the maximum lateral soil spring force per unit length of pipe,  $\Delta_p$  the yielding displacement of lateral soil spring.

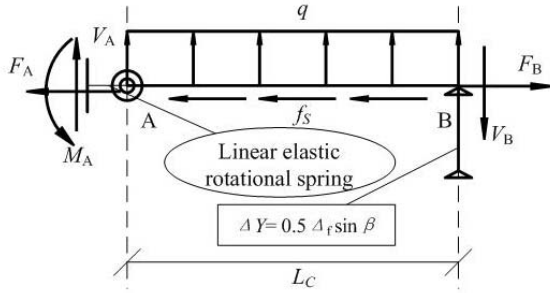


**Figure 4.** Sketch of elastic-beam theory in segment AB

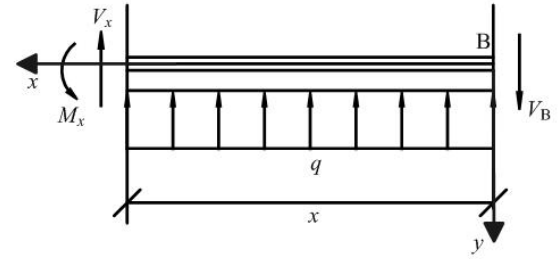


**Figure 5.** Sketch of bending analysis for elastic-beam segment

Using the elastic-beam theory, the expressions for  $M_A$ ,  $V_A$  and  $V_B$  are obtained:

$$M_A = \frac{12E_{\tan} I \Delta_f C \sin \beta - qCL_C^4}{24E_{\tan} IL_C + 8CL_C^2} \quad (3.15)$$

$$V_A = \frac{12E_{\tan} I \Delta_f C \sin \beta - 12E_{\tan} I qL_C^3 - 5qCL_C^4}{24E_{\tan} IL_C^2 + 8CL_C^3} \quad (3.16)$$

$$V_B = \frac{12E_{\tan} I \Delta_f C \sin \beta + 12E_{\tan} I qL_C^3 + 3qCL_C^4}{24E_{\tan} IL_C^2 + 8CL_C^3} \quad (3.17)$$

where  $E_{\tan}$  is the tangent Young's modulus of Ramberg-Osgood model for pipe steel corresponding to the maximum axial total stress, which can be obtained by Eq.(2.2), and  $V_B$  is the shear force at point B.

## 3.4 Determination of pipe maximum axial total stress

### 3.4.1 Bending stress analysis

Based on the equilibrium equation of bending moment, the bending stress  $\sigma_{x1}$  at any point for the segment  $0 \leq x \leq L_C$  shown in Figure 5 can be taken:

$$\sigma_{x1} = \frac{M_x D}{2I} = \frac{DV_B}{2I} x - \frac{Dq}{4I} x^2 \quad (3.18)$$

where  $M_x$  is the bending moment of arbitrary point in the segment  $0 \leq x \leq L_C$ .

Due to  $\sigma'_{x1} = 0$  and  $\sigma''_{x1} = -\frac{Dq}{2I} < 0$ , the position of pipe maximum bending stress is obtained as  $x_{\text{bend}} = \frac{V_B}{q}$ . Substitute into Eq. (3.18), then the pipe maximum bending stress is obtained as:

$$\sigma_{x1\text{bend}} = \frac{DV_B}{2I} x_{\text{bend}} - \frac{Dq}{4I} x_{\text{bend}}^2 \quad (3.19)$$

Based on the derivation from Eq. 18 and Eq. 19,  $0 \leq x_{\text{bend}} \leq L_C$  must exist, i.e. the maximum bending stress position is in the elastic-beam segment.

### 3.4.2 Axial stress analysis

For the axial stress analysis, two cases are classified based on the yielding condition of the axial soil springs. For case 1, the axial soil springs of segment  $L_C$  are still elastic (Figure 6). Referred to the coordinate system of Figure 6, the axial total stress  $\sigma_t$  of arbitrary point in the segment  $L_C$  is expressed as:

$$\sigma_t = \sigma_{ax} + \sigma_{x1} = \frac{f_s(x-L)^2}{2A_s L_0} + \frac{DV_B}{2I} x - \frac{Dq}{4I} x^2 \quad (3.20)$$

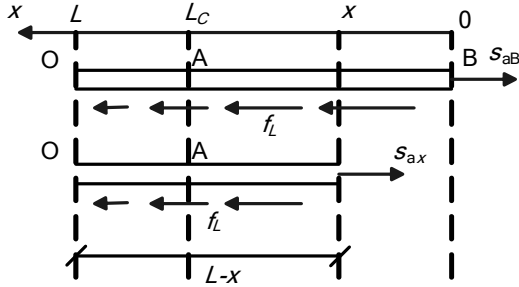


**Figure 6.** Sketch of axial analysis in elastic-beam segment with axial soil springs not yielding

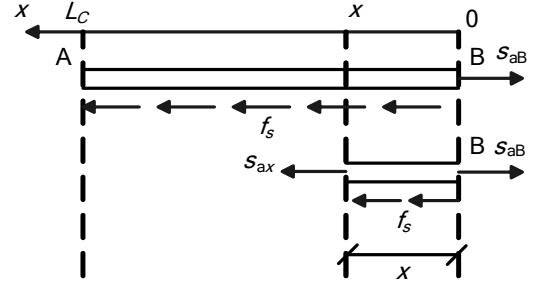


**Figure 7.** Sketch of axial analysis in elastic-beam segment with axial soil springs yielding

Since the axial soil springs are elastic along the whole pipeline, the bending stress  $\sigma_{x1}$  is dominant compared with the axial stress  $\sigma_{ax}$ . According to  $\sigma'_t = 0$  and  $\sigma''_t < 0$ , the position of pipe maximum axial total stress is determined, then the maximum axial total stress of pipeline is obtained as:

$$\sigma_{t\text{max}} = \frac{f_s(x_{\text{max}} - L)^2}{2A_s L_0} + \frac{DV_B}{2I} x_{\text{max}} - \frac{Dq}{4I} x_{\text{max}}^2 \quad (3.21)$$

For case 2, the axial soil springs yield totally. Since segment AB is close to the intersection of the pipeline axis with the fault trace and very short, the axial soil springs of the segment are assumed to yield (Figure 7). By superposition of the bending and axial stresses, the axial total stress  $\sigma_t$  of arbitrary point in segment  $L_C$  is expressed as:

$$\sigma_t = \sigma_{ax} + \sigma_{x1} = \sigma_{aB} - \frac{f_s}{A_s} x + \frac{DV_B}{2I} x - \frac{Dq}{4I} x^2 \quad (3.22)$$

Based on  $\sigma_t' = 0$  and  $\sigma_t'' = -\frac{Dq}{2I} < 0$ , the position of pipe maximum axial total stress is obtained, then the maximum axial total stress of pipeline is calculated as:

$$\sigma_{t \max} = \sigma_{aB} - \frac{f_s}{A_s} x_{\max} + \frac{DV_B}{2I} x_{\max} - \frac{Dq}{4I} x_{\max}^2 \quad (3.23)$$

From the further analysis,  $0 \leq x_{\max} \leq x_{\text{bend}} = \frac{V_B}{q}$  exists, i.e. the position of pipe maximum axial total stress locates between the maximum-bending-stress point and the maximum-axial-stress point.

## 4 VALIDATION AND EXAMPLE ANALYSIS

### 4.1 Validation of proposed methodology

To validate the proposed methodology, analytical predictions are compared with the results from Karamitros method and three-dimensional non-linear FE analyses using ADINA (2008). The pipe-shell element length is 1 m, and each element has 4 nodes. To simulate pipe-soil nonlinear interaction, two ends of each element are connected to axial, lateral and vertical soil springs modeled as elastic perfectly-plastic spring elements.

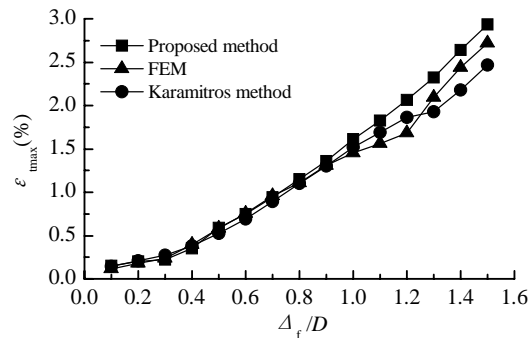


**Figure 8.** Effects of fault displacements on pipe maximum axial total strain

Based on the parameters of Karamitros's paper (2006), the results from FEM, Karamitros method and proposed method are shown in Figure 8. With increasing fault displacements, the pipe maximum axial total strains from Karamitros method are less than those from numerical method and non-conservative, while the results from the proposed method are in better agreement with those from numerical method and conservative at the larger fault displacements.

### 4.2 Effects of seabed soils

A submarine buried steel pipeline is selected, featuring the outside diameter of 1.32 m, the wall thickness of 19.06 mm, and the total length of 1200 m. The pipe steel is the API SPEC 5L X60 type, and the properties from the Indian standard (2007) are listed in Table 4.1.

The properties of soil springs are calculated according to the ALA guidelines (2001) listed in Table 4.2, assuming that the pipeline centerline is buried under 1.98 m of silty sand with cohesion 0 kPa, internal friction angle  $33^\circ$  and unit weight  $19.2 \text{ kN/m}^3$ , which is a typical shallow seabed soil. Another two typical shallow seabed soils are adopted as follow: the very soft silty clay with cohesion 14

kPa, internal friction angle  $0^\circ$  and unit weight  $17.5 \text{ kN/m}^3$  and the clay with cohesion  $42 \text{ kPa}$ , internal friction angle  $0^\circ$  and unit weight  $17.29 \text{ kN/m}^3$ . The coating dependent factor relating the internal friction angle of the soil to the friction angle at the soil-pipe interface  $f$  is  $0.7$ . The fault movement  $\Delta_f = 10 \text{ m}$  is statically applied with the crossing angle,  $\beta = 30^\circ$  and  $70^\circ$ , respectively.

**Table 4.1.** Parameters of Ramberg-Osgood stress-strain curve for API SPEC 5L X60 pipe steel

Parameters	Values
Initial Young's modulus ( $E_0$ )	$2.1e5 \text{ MPa}$
Yielding stress ( $\sigma_y$ )	$413 \text{ MPa}$
$n$	10
$r$	12

**Table 4.2.** Soil spring properties

Soil kinds	Soil spring parameters	Yielding force N/m	Yielding displacement m
silty sand	Axial soil springs	$2.42e4$	$4.00e-3$
	Transverse soil springs	$1.98e5$	$1.06e-1$
	Vertical uplift soil springs	$2.71e4$	$2.97e-2$
	Vertical bearing soil springs	$1.15e6$	$1.32e-1$
Very soft silty clay	Axial soil springs	$5.90e4$	$9.00e-3$
	Transverse soil springs	$1.02e5$	$1.06e-1$
	Vertical uplift soil springs	$5.55e4$	$2.64e-1$
	Vertical bearing soil springs	$1.16e5$	$2.64e-1$
Clay	Axial soil springs	$1.69e5$	$8.00e-3$
	Transverse soil springs	$3.07e5$	$1.06e-1$
	Vertical uplift soil springs	$1.66e5$	$1.98e-1$
	Vertical bearing soil springs	$3.06e5$	$2.64e-1$

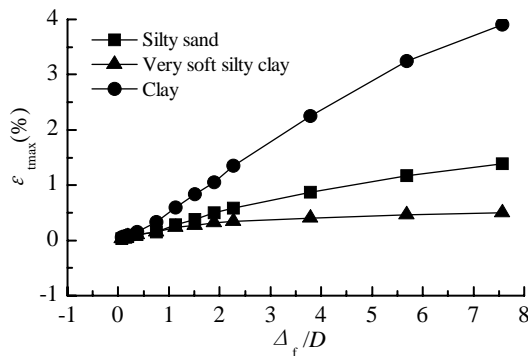


**Figure 9.** Effects of fault displacements on pipe maximum axial total strain ( $\beta = 30^\circ$ )

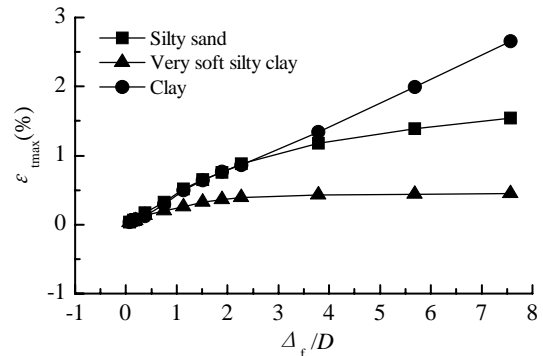


**Figure 10.** Effects of fault displacements on pipe maximum axial total strain ( $\beta = 70^\circ$ )

For the three typical shallow seabed soils, the variations of pipe maximum axial total strains with fault displacements from the proposed methodology are displayed in Fig. 9 and Fig. 10. With increasing fault displacements, the peak values of pipe axial total strain are very different for the different seabed soils. Compared with the silty sand and very soft silty clay, the peak values of pipe axial total strain for clay site are largest due to the strongest constraints on pipelines and pipe-soil interaction, and it goes against the seismic resistance of submarine buried steel pipelines across strike-slip faults.

## 5 CONCLUSIONS

Considering the nonlinearity of soil-pipeline interaction, an improved analytical methodology of submarine buried steel pipelines surrounded by homogeneous site soils across active strike-slip faults

is proposed in the paper. Based on the beam-on-elastic-foundation and elastic-beam theories, the pipe maximum axial total stress and strain are derived.

Compared with Karamitros method, the pipe maximum axial total strains from the proposed analytical methodology are in better agreement with the FE ones and suitable for engineering applications due to conservative results.

## ACKNOWLEDGEMENTS

The research was supported by Ministry of Science and Technology of China (Grant No. 2011CB013702). This research was also supported by the Fundamental Research Funds for the Central Universities (Grant No. DUT10ZD201). Their financial supports are gratefully acknowledged.

## REFERENCES

- Gu, X. T. and Zhang, H. (2009). Research on aseismic measures of gas pipeline crossing a fault for strain-based design. *ASME Pressure Vessels and Piping Conference*, Vol. 7: 571-580.
- Jiao, Z. L., Shuai, J. and Han, K. J. (2009). Response analysis of buried pipeline subjected to fault movements. *International Conference on Pipelines and Trenchless Technology: Advances and Experiences with Pipelines and Trenchless Technology for Water, Sewer, Gas, and Oil Applications*. Vol. 10: 1212-1218.
- Liu, M., Wang, Y. Y. and Yu, Z. F. (2008). Response of pipelines under fault crossing. *International Offshore and Polar Engineering Conference*. Vol. 7: 162-165.
- Vazouras, P., Karamanos, S. A. and Dakoulas, P. (2010). Finite element analysis of buried steel pipelines under strike-slip fault displacements. *Soil Dynamics and Earthquake Engineering*. 30: 11, 1361-1376.
- Newmark, N. M. and Hall, W. J. (1975). Pipeline design to resist large fault displacement. *US conference on earthquake engineering*. Vol. 6: 416-425.
- Kennedy, R. P., Chow, A. W. and Williamson, R. A. (1977). Fault movement effects on buried oil pipeline. *Transportation Engineering Journal*, 103: TE5, 617-633.
- Wang, R. L. and Yeh, Y. H. (1985). A refined seismic analysis and design of buried pipeline for fault movement. *Earthquake Engineering and Structural Dynamics*, 13: 75-96.
- Karamitros, D. K., Bouckovalas, G. D. and Kouretzis, G. P. (2006). Stress analysis of buried steel pipelines at strike-slip fault crossings. *Soil Dynamics and Earthquake Engineering*, 27: 200-211.
- American Lifeline Alliance. (2001). Guidelines for the design of buried steel pipe. *American Society of Civil Engineers*.
- Indian Institute of Technology Kanpur, Gujarat State Disaster Management Authority. (2007). IITK-GSDMA, Guidelines for seismic design of buried pipelines: provisions with commentary and explanatory examples. India: National Information Center of Earthquake.
- ADINA R D Lnc. (2008). ADINA Theory and Modeling Guide. Watertown, USA: ADINA R D, Lnc., Vol. I: 147-165.